Quantitative Measurement of Chain Contraction in a Solid Blend of Two Incompatible Polymers: Poly(methyl methacrylate)/Poly(vinyl acetate)

Kristen A. Peterson, Alan D. Stein, and M. D. Fayer*

Department of Chemistry, Stanford University, Stanford, California 94305.
Received January 30, 1989; Revised Manuscript Received May 23, 1989

ABSTRACT: Electronic excitation transport among naphthyl chromophores in low concentration on isolated chains of poly(2-vinylnaphthalene-*co*-methyl methacrylate) dispersed in both poly(methyl methacrylate) (PMMA) and poly(vinyl acetate) (PVAc) is monitored by time-resolved fluorescence depolarization spectroscopy. Analysis of the results with a theory for excitation transport in finite volume systems utilizing a Gaussian segment distribution function allows the quantitative determination of the root-mean-square radius of gyration ($\langle R_g^2 \rangle^{1/2}$) of PMMA in the two hosts. The results for bulk PMMA agree with expected values for PMMA in a Θ solvent. The naphthyl groups do not perturb the average chain conformation. A significant decrease in $\langle R_g^2 \rangle^{1/2}$ for isolated PMMA chains is observed in the PMMA/PVAc blend. These are the first measurements of $\langle R_g^2 \rangle^{1/2}$ and chain collapse in a solid blend of two incompatible polymers. At higher concentrations of PMMA in PVAc, micro-phase separation on the order of aggregation of two or three chains is observed.

I. Introduction

There is significant interest in characterizing solid polymeric materials, especially blends, at the molecular level. This interest is due, in large part, to the tremendous technological importance of polymer blends. The bulk, macroscopic properties of such materials are determined by the microscopic structure which, in turn, is critically dependent on the degree of molecular mixing between blend components. The special properties of polymer materials arise from differences between the thermodynamic interactions in systems containing macromolecules and those in systems of only small molecules.

The nature of intermolecular interactions determines the microscopic structure in any condensed-phase system. However, when macromolecules are involved, there is additional complexity due to intramolecular considerations; the number of configurations available to a polymer chain, although restricted by covalent bond geometries, is vast. Thus, the morphology of a chain involves the interplay between the interactions of the polymer with its environment and the possible chain conformations. To understand these systems more fully, it is desirable to investigate quantitatively the interactions of isolated

* To whom correspondence should be addressed.

0024-9297/90/2223-0111$02.50/0

polymer chains with the host environment.

Techniques that exploit the phenomenon of incoherent electronic excitation transport are becoming increasingly powerful in the study of polymer systems. In the past several years, a number of studies have made use of the dependence of excitation transport on local chromophore concentration to provide qualitative information on polymer miscibility and phase separation, the degree of chain entanglement, kinetics of spinodal decomposition, and chain conformation.[1-3] These studies involved a variety of transport events: donor to donor, monomer to excimer, and donor to acceptor transfer. More recently, due to advances in the theoretical description of excitation transport in nonrandom and finite volume systems,[4,5] interest has developed in using this phenomenon to obtain quantitative information on average chain conformation, intrachain geometry, and also domain size in phase-separated systems.

Recently, the first quantitative measurements of average chain conformation were made by using an electronic excitation transport technique. Previous publications described an experimental method,[6,7] time-resolved fluorescence depolarization spectroscopy, for measuring the rate of excitation transport among chromophores attached to polymer chains and a mathematical model[8] of the process that allows the extraction of quantitative size information on the molecular scale. Data were presented which conclusively demonstrated that it is possible to measure the ensemble averaged root-mean-square radius of gyration, $\langle R_g^2 \rangle^{1/2}$, of polymer chains in the amorphous solid state via such experiments. In that study,[7] the $\langle R_g^2 \rangle^{1/2}$ of atactic poly(methyl methacrylate) (PMMA) in the bulk was determined, the results being equivalent to determinations by light scattering in Θ solvents and by neutron scattering in the bulk. Thus, the feasibility of using excitation transport techniques to study quantitatively the molecular interactions in solid polymer blends by measurement of the average chain conformation was demonstrated.

Here, we present the results of experiments that monitor the rate of excitation transport among chromophores (2-vinylnaphthalene) on isolated guest chains (PMMA) in a host polymer of a different type: poly(vinyl acetate) (PVAc). The data show a clear decrease in $\langle R_g^2 \rangle^{1/2}$ for PMMA chains in PVAc relative to the value in bulk PMMA. This decrease is a direct measure of the strength of the thermodynamic interactions between the two polymers.

In addition, concentration studies show that the technique is extremely sensitive in detecting micro-phase separation on the order of aggregation of two or three chains. There is also evidence that a small increase (~15%) in the degree of polymerization of the guest polymer affects the critical concentration for phase separation.

The qualitative relationship between excitation transport dynamics and the volume occupied by a polymer chain (characterized, for example, by $\langle R_g^2 \rangle^{1/2}$) is straightforward. Consider an ensemble of polymer chains, with a small number of chromophores bound to the chains, dispersed in a host matrix at low enough concentration that the chromophore tagged chains are isolated from each other. These chains will have an $\langle R_g^2 \rangle^{1/2}$ determined by the guest–host interactions. If the guest chains are dispersed in a host polymer with which they have favorable thermodynamic interactions, they will assume extended configurations with a large average interchromophore separation. Since the rate of excitation transport is a strong function of distance (proportional to $1/r^6$ where r is the chromophore separation), an extended conformation results in a relatively slow rate of excitation transport. Conversely, if the same guest polymer is placed in a different host, where thermodynamic interactions are less favorable, the chains will contract, resulting in more rapid excitation transport. The $1/r^6$ distance dependence makes excitation transport observables very sensitive to small changes in $\langle R_g^2 \rangle^{1/2}$. Clearly, an experiment that monitors the rate of excitation transport among chromophores on polymer chains should provide a direct measure of chain size and polymer–polymer interactions. A detailed description of the relationship between $\langle R_g^2 \rangle^{1/2}$ and experimental observables is given in section II.

Motivation for using excitation transport phenomena for investigating the structure of polymer blends comes, in part, from the limitations of other techniques. Light scattering has been used extensively to measure $\langle R_g^2 \rangle^{1/2}$ in good and Θ solvents.[9] Recent experiments have measured chain collapse as a dilute polymer solution is lowered below the Θ temperature.[10,11] However, this method cannot be applied to solids.

The most common experimental method used to determine $\langle R_g^2 \rangle^{1/2}$ of isolated polymer chains in solid blends is small-angle neutron scattering (SANS). Although this technique has yielded considerable insights into the nature of polymeric solids, providing direct measurement of chain size in bulk[12,13] and in miscible blends,[14-16] it has a few disadvantages. First, due to scattering from the host, it is difficult to investigate the behavior of the guest polymer at very low concentrations (<1%). This limitation is of particular importance since many polymer blends are phase-separated even at this relatively low concentration. Excitation transport can be detected by fluorescence techniques. Since fluorescence is detected against a dark background, it can be used to investigate the properties of a minor component at concentrations several orders of magnitude lower than is possible in a neutron scattering experiment. Second, in a SANS experiment, to produce contrast one of the blend components must be deuterated. Deuteration has been shown to affect the thermodynamic properties of a number of polymer systems.[17-19] Assessing the effect of deuteration on neutron scattering results, although possible, is quite difficult.[19b,20] As has been discussed in detail elsewhere,[7] although it is possible that the introduction of chromophores into a polymer system for excitation transport experiments can have an effect on the guest–host interactions, the detection and removal of any such effects is handled easily through extrapolation to zero tagging fraction. Finally, the monochromatic neutron source required is much less accessible than the commercially available equipment needed for the experiments described here.

Small-angle X-ray scattering (SAXS) has also been employed in the study of miscible polymer blends[21] but is limited to mixtures of the few polymers that exhibit a large enough scattering contrast to allow accurate measurements. In addition, SAXS, like SANS, cannot be applied to studying isolated guest chains in immiscible blends due to poor signal to background at very low concentrations.

The detection of excitation transport via time-resolved fluorescence depolarization spectroscopy is an extremely flexible tool for studying structure on a microscopic scale. It can be used for many of the same studies of polymeric solids as neutron scattering, provided the host material's optical properties are compatible with detection of fluorescence from the guest polymer. Exci-

tation transport experiments are unique however, as they allow the study of both miscible and immiscible blends. The results presented below provide the first measurement of average chain conformation in a solid blend of two incompatible polymers.

II. Experimental Observables

In systems involving donor–donor excited-state transport, the fundamental quantity of theoretical and experimental interest is $G^s(t)$; the ensemble-averaged probability that an originally excited chromophore is excited at time t.[22] $G^s(t)$ contains contributions from excitations that never leave the originally excited chromophore and from excitations that return to the initially excited chromophore after one or more transfer events. $G^s(t)$ does not contain loss of excitation due to lifetime (fluorescence) events. In this section we discuss how $G^s(t)$ can be obtained experimentally from time-resolved fluorescence depolarization data. The method used to calculate the theoretical $G^s(t)$ and its relationship to $\langle R_g^2\rangle^{1/2}$ are also briefly described.

If a sample of randomly oriented chromophores is excited by a short pulse of plane polarized light, the decay of the fluorescence intensities polarized parallel ($I_\parallel(t)$) and perpendicular ($I_\perp(t)$) to the exciting light can be written as

$$I_\parallel(t) = e^{-t/\tau}(1 + 2r(t))$$
$$I_\perp(t) = e^{-t/\tau}(1 - r(t)) \quad (1)$$

τ is the fluorescence lifetime, and $r(t)$ is the fluorescence anisotropy. $r(t)$ contains information about all sources of depolarization. If the transition dipoles of the chromophores in a solid polymer matrix are randomly oriented, the main source of depolarization in these experiments will be due to excitation transport. The initially excited ensemble is polarized along the direction of the excitation $\vec{E}$ field and gives rise to polarized fluorescence. Transport occurs into an ensemble of chromophores with randomly distributed dipole directions, and the fluorescence becomes unpolarized. The random distribution of directions is assured by the low concentration of chromophores on the tagged chains. To a slight extent, on the time scale of interest, depolarization also occurs as a result of chromophore motion. In this case the fluorescence anisotropy is approximately

$$r(t) = C\Phi(t)G^s(t) \quad (2)$$

where $\Phi(t)$ is the rotational correlation function that contains the effects due to motion of the chromophores. C is a time-independent constant that describes the degree of polarization of the excitation and emission transitions involved. There are two approximations in eq 2. The first is that the rotational and energy transport contributions to depolarization are independent. This is an excellent approximation for the very slow and small extent of rotational depolarization in polymer blends below the glass transition temperature, as is the case for the blends in this study. This may not be applicable to more fluid systems such as polymer melts. Fredrickson has recently treated the case where energy transport and rotation occur on similar time scales.[23]

The second approximation is that $G^s(t)$ decays to zero resulting in complete depolarization; i.e., the irreversible transfer of excitation from the initially excited donor into the ensemble of unexcited donors results in total loss of polarization. For chains with a low concentration of randomly placed chromophores this is approximately true. The residual polarization following a single transfer event is only 4%, which results in an insignificant error.[24]

To obtain $G^s(t)$ for a given polymer, experiments on two different samples must be performed. These samples differ only in that the guest copolymers have a different fraction of chromophore containing monomers. Copolymer A is the polymer of interest and has an appreciable number of chromophores, such that excitation transport will occur. Its fluorescence anisotropy, $r_A(t)$, is given by eq 2. Copolymer B has such a small number of chromophores that excitation transport is negligible ($G^s(t) = 1$) and only chromophore motion contributes to the anisotropy

$$r_B(t) = C\Phi(t) \quad (3)$$

$G^s(t)$ arising from the excitation transport on copolymer A can be calculated from the two experimental anisotropies:

$$G^s(t) = r_A(t)/r_B(t) \quad (4)$$

This method of determining $G^s(t)$ has the advantage that detailed knowledge of the parameters C and $\Phi(t)$ is unnecessary. $r(t)$ for either copolymer can be obtained from the individual parallel and perpendicular components of the fluorescence intensity. From eq 1

$$r(t) = \frac{I_\parallel(t) - I_\perp(t)}{I_\parallel(t) + 2I_\perp(t)} \quad (5)$$

The denominator in eq 5 divides out the population decay whether it is exponential as shown in eq 1 or not. Thus $r(t)$ is independent of the population kinetics.

To obtain a value for $\langle R_g^2\rangle^{1/2}$ of copolymer A, we compare the experimentally determined $G^s(t)$ to a theoretical calculation of $G^s(t)$ for the copolymer. Once the molecular weight and number of chromophores are known (these can be independently determined), the theory has only one adjustable parameter, the statistical segment length. This parameter is directly related to $\langle R_g^2\rangle^{1/2}$.

The theory employed to analyze the data presented here has been described in detail elsewhere.[8] Only a brief summary and the pertinent equations will be given here. Random flight statistics with an appropriate statistical segment length are employed to describe the average chain conformation of the copolymer chains. This model has been applied successfully to polymer coils in solution.[25] For a polymer with chromophores randomly distributed along the chain, the chromophore distribution function can be modeled by

$$P_i(r_{12})\,d\vec{r}_{12} = 4\pi r_{12}^2\left\{np'(r_{12}) + \frac{(N-n-1)}{(\bar{N}-1)}\sum_{\substack{j=1\\ j\neq i}}^{\bar{N}}\left(\frac{3}{2\pi a^2|i-j|}\right)^{3/2}\exp\left(\frac{-3r_{12}^2}{2a^2|i-j|}\right)\right\}dr_{12} \quad (6)$$

Equation 6 describes the probability that a chromophore (labeled 2) on any chain segment j is a distance r_{12} from a chromophore (labeled 1) on chain segment i. $\bar{N}$ and a are the number of statistical segments and the statistical segment length of the polymer, respectively. N is the total number of chromophores on the chain, and n is the average number of unexcited chromophores also on segment i.

The second term on the right-hand side of eq 6 gives the contribution to the chromophore density at r_{12} from all chromophores not on segment i. The first term models the chromophore distribution ($p'(r_{12})$) around chromophore 1 due to other chromophores also on segment i. For the low tagging percentages used in the experi-

ments, this is a very small contribution to the overall distribution function. It is mainly included to preserve normalization, and its form is not critical.[8] Therefore, we use a simple approximation for this distribution, assuming chromophore 1 is in the center of the segment and the other n chromophores are distributed randomly about this point:

$$p'(r_{12}) = 1/A \qquad 0 \le r_{12} \le a/2 \tag{7}$$
$$p'(r_{12}) = 0 \qquad r_{12} > a/2$$

where A is the volume of a sphere of radius $a/2$.[26]

Excited-state transport has been described by using many theoretical formalisms.[22,27-29] The theory we employ to describe the rate of excitation transport among the chromophores on a finite length polymer chain is an adaptation of a first-order cumulant expansion method developed by Huber for isotropic solutions.[29] The problem of excitation transport among chromophores randomly tagged in low concentration on a finite length polymer chain is a finite volume problem.[4,5] Excitation transport in various finite volume systems has been treated by this formalism.[8,30] Initial excitation of a chromophore near the edge of the region occupied by a chain results in different dynamics than excitation of a chromophore near the middle of the region because of the different distributions of chromophores about these two points.

In treating the problem of excitation transport dynamics in finite volume systems, it is necessary to perform two spatial averages. The first is an average over all the possible configurations of the other chromophores about the location of the initially excited chromophore (in this case located on polymer segment i). This results in an expression for $G^s_i(t)$, which describes the excitation transport arising from this initial excitation condition. The second average is over all the possible locations for the initial excitation which, in a finite volume problem, are not all equivalent. For this polymer model, this amounts to a sum over the chain segments.

Peterson and Fayer have applied the first-order cumulant expansion to this problem. The details of the calculations and demonstrations of its accuracy are reported in ref 8. These investigators apply the cumulant expansion to $G^s_i(t)$, and then, within the context of the freely jointed chain model, they perform the average over the position of initial excitation exactly. This results in a more accurate approximation than applying the cumulant expansion to $G^s(t)$ directly, since it avoids the approximate average over the initial location of excitation.

Using the chromophore distribution function, $P_i(r_{12})$, performing the cumulant expansion, and then averaging over the possible positions of the initially excited chromophore, we obtained an expression for $G^s(t)$.

$$G^s(t) = \frac{1}{N}\sum_{i=1}^{N} \exp\left[\frac{4\pi}{2}\int_0^\infty (e^{-2\omega_{12}t} - 1)P_i(r_{12})r_{12}^2\, dr_{12}\right] \tag{8}$$

ω_{12} is the rate of excitation transport between two chromophores at a separation of r_{12}. In eq 8, the exponential term is $G^s_i(t)$ and the sum over i (chain segments) is the average over the initial positions of excitation.

For rapidly rotating chromophores ω_{12} is given by[27]

$$\omega_{12} = (R_0/r_{12})^6/\tau \tag{9}$$

τ is the fluorescence lifetime, and R_0 is the critical transfer radius. Equation 9 is the orientation-averaged expression for dipole–dipole interactions and is applicable to dynamic systems (e.g., chromophores in solution). For the experiments in this paper, the chromophores are essentially static and R_0 in eq 9 must be replaced by

$$R_0' = (\gamma_2)^{1/3}R_0 \tag{10}$$

where $\gamma_2 = 0.8468$.[31]

Provided the molecular weight and the percent tagging of the copolymer is known, eq 8 has only one adjustable parameter: the statistical segment length a. This is directly related to $\langle R_g^2\rangle^{1/2}$ by

$$\langle R_g^2\rangle = (1/6)(\bar{N}a^2) \tag{11}$$

Thus, a fit of the experimentally determined $G^s(t)$ with a theoretically calculated $G^s(t)$ determined by adjusting the statistical segment length, and convolved with the instrument response, will give a measure of $\langle R_g^2\rangle^{1/2}$ for the copolymer.

Table I
Copolymer Characteristics

copolymer	mole fractn 2-VN	mol wt	M_w/M_n	av no. of chromophores/chain
I	0.0015	~50 000	~2.5	<1
4-26	0.040	26 000	1.2	10 ± 1
9-22	0.087	22 700	1.3	20 ± 1

III. Experimental Section

A. Polymer Materials. Three copolymers of methyl methacrylate (MMA) and 2-vinylnaphthalene (2-VN) were used in the fluorescence depolarization experiments. Two contained a high enough fraction of 2-VN (0.087 and 0.040 mole fractions) to have fluorescence depolarization due to both excitation transport and molecular motion. The third had a very small fraction of 2-VN monomers (0.0015 mole fraction) and was used to assess depolarization due to chromophore motion and time-independent sources. All were polymerized in benzene at 60 °C under nitrogen following the procedure of Fox et al.[32] AIBN and butanethiol were used as initiator and chain-transfer reagent, respectively. The MMA (Aldrich) was washed with 5% NaOH, dried over Na_2SO_4, and vacuum distilled. The 2-VN (Aldrich) was recrystallized three times from ethanol and sublimed once. The AIBN was recrystallized from ethyl acetate. The copolymers were recovered from the reaction mixture by precipitation into methanol and subsequently washed several times with cold methanol. 2-Ethylnaphthalene (2-EN, Aldrich) was employed as the chromophore in the samples used to determine R_0.

The desired molecular weight fractions were obtained from the resulting polydisperse copolymers by size exclusion chromatography using Sephacryl S-200 resin and THF as eluent. The molecular weights of the fractions were determined on a Waters Associates analytical GPC using THF as eluent. The GPC instrument was calibrated by using nearly monodisperse PMMA standards (Pressure Chemical, $M_w/M_n < 1.1$). The copolymer used to determine the depolarization due to chromphore motion (0.0015 mole fraction 2-VN) was not fractionated. Its average molecular weight was determined by viscosity measurements. The mole fractions of vinylnaphthalene monomer units in the copolymers were determined by absorption spectroscopy in THF solution at 320 nm (Cary 17 spectrometer), based on a molar extinction coefficient of 400 mol·cm/L measured for 2-ethylnaphthalene in THF. Table I gives a summary of the characteristics of the three copolymers. The host polymers for the blends were the following: (1) PMMA, Pressure Chemical Co., Lot PM6-2 molecular weight 61 800, $M_w/M_n = 1.1$; (2) PVAc, Aldrich 18,248-6 high molecular weight (GPC average ~ 167 000).

B. Sample Preparation. All samples were solid blends of the desired guest molecule (tagged polymer or 2-EN) and the host polymer, prepared by molding in a stainless-steel piston above the glass transition temperature (T_g). The mixtures used for molding were prepared by freeze-drying a solution (less than 5% solids in benzene) of the components in the desired ratio. Some type of thermal decomposition that caused a significant amount of background fluorescence was observed when the

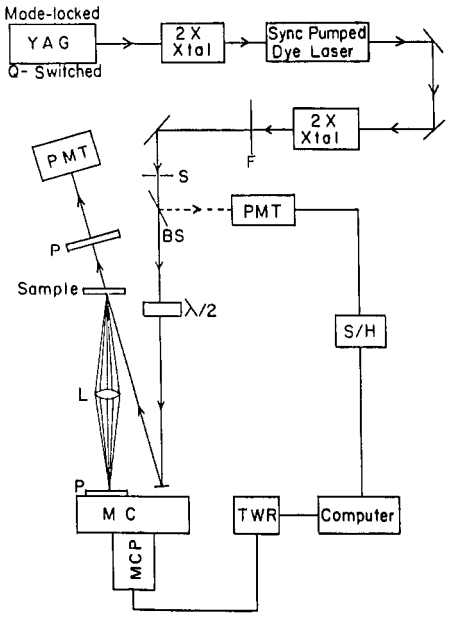

Figure 1. Experimental apparatus for time-resolved fluorescence depolarization spectroscopy. The output of a mode-locked and Q-switched Nd:YAG laser is frequency doubled and synchronously pumps a dye laser. The dye laser output is doubled to 320 nm for excitation. The polarization of the excitation beam is controlled by an acoustooptic half-wave plate. A beam splitter sends a small part of the excitation beam to a phototube for normalization. The polarizer and phototube after the sample were in place only when the polarization ratio was measured through the sample. The fluorescence from the sample is collected by a lens, passed through a polarizer and a monochromator, and detected by a microchannel plate coupled to a transient digitizer. See text for further details. Abbreviations: S, mechanical shutter; BS, beam splitter; PMT, photomultiplier tube; λ/2, half-wave plate; S/H, sample and hold circuit; P, polarizer, L, lens; MC, monochromator; MCP, microchannel plate detector; TWR, transient waveform recorder; F, UV transmitting filter; 2 × Xtal, second harmonic generating crystal.

PMMA samples were molded in the presence of oxygen. For this reason, all the samples were molded either under vacuum or, in the case of those containing 2-EN, under a nitrogen atmosphere slightly above ambient pressure. This was necessary to avoid excessive loss of the 2-EN at elevated temperatures.

The thickness of the samples was chosen to ensure the optical density at 320 nm was less than 0.2. Due to differences in T_g, the molding procedure for the two host polymers differed somewhat and were as follows:

(1) PMMA (T_g = 104 °C). The piston apparatus was heated to 125–130 °C during a period of 20–30 min and held at this temperature for 20 min. A pressure of 0.8 metric ton (piston surface area was a circle of 1-cm diameter) was applied for 1 min and released. The temperature is held at 125–130 °C for 20 min, and a pressure of 0.8 metric ton was again applied for 1 min and released. The apparatus was then allowed to cool and was held at 100–105 °C for 15 min and then cooled slowly to room temperature.

(2) PVAc (T_g = 30 °C). The piston apparatus was heated to 88–92 °C over a period of 20–30 min and held at this temperature for 30 min. A pressure of 0.5 metric ton was then applied for 1 min and released. The apparatus was allowed to cool to 70–73 °C and then pressed at 0.8 metric ton for 1 min. The temperature was maintained at 70–73 °C for 15 min and then allowed to return slowly to room temperature.

C. Data Acquisition. Figure 1 shows the experimental apparatus. The frequency-doubled (532 nm) output of an acoustooptically mode-locked, Q-switched Nd:YAG laser was used to synchronously pump a dye laser. The dye laser was cavity dumped with a Pockels cell to produce a single pulse at 640 nm that was then frequency-doubled to give the ~25-ps excitation pulse at 320 nm. This was at the peak of the absorption of the first excited singlet state of the naphthyl chromophores. A small fraction of each UV excitation pulse was measured with a phototube and sample-and-hold circuit and recorded by computer, normalizing the fluorescence intensity to the laser intensity. This eliminated effects due to laser intensity drift. Fluorescence from the sample was focused into a monochromator tuned to 337 nm with a polarizer on the entrance slit. A microchannel plate (Hamamatsu R1645U-01) coupled to a transient digitizer (Tektronix model R7912) detected the fluorescence. A computer was used to store the fluorescence decays and average many decays (500–2000 per data set) to improve signal-to-noise. The time resolution of the detection system, measured by detecting scattered light from the excitation pulse, was 1.3 ns.

The spot size of the excitation pulse at the sample was of the order of 1-mm diameter, and the pulse energies were typically 0.5–1 μJ. Careful experimental examination of samples of various concentration demonstrated that no significant reabsorption of fluorescence occurred. The dependence of the recorded fluorescence intensity on the excitation intensity was linear, assuring that the microchannel plate was not saturated and that the sample was not being bleached.

The intensities for fluorescence polarized parallel to the excitation polarization, $I_{\parallel}(t)$, and fluorescence polarized perpendicular to the excitation polarization, $I_{\perp}(t)$, were measured by rotating the polarization of the excitation pulse with an electrooptic half-wave plate (Pockels cell) and keeping the detector polarizer unchanged at vertical polarization. Since the detection efficiency of the monochromator and microchannel plate can vary with the polarization of the light, this method ensured that the absolute ratio of $I_{\parallel}(t)$ to $I_{\perp}(t)$ was preserved. Front face excitation and detection were used.

A mechanical shutter before the sample blocked every other laser shot, allowing both a signal and background shot to be taken at each polarization. A computer-controlled circuit switched the half-wave voltage on or off after each signal shot. This resulted in an alternation of the excitation polarization between parallel and perpendicular. Two data sets, $I_{\parallel}(t)$ = $I_{\parallel}$(signal) − $I_{\parallel}$(background) and similarly for $I_{\perp}(t)$, were stored as running averages by the computer. The fluorescence anisotropy $r(t)$ (see next section) was then calculated from this set of $I_{\parallel}(t)$ and $I_{\perp}(t)$ decays after normalizing to the laser intensity. The entire sequence was repeated for the same spot and different spots on the same sample. No substantial or systematic differences were observed. The $r(t)$ curves calculated from these separate data sets were then averaged together. Switching back and forth between collecting fluorescence at the two polarizations minimized any possible artifacts.

In addition to checking the birefringence of the samples with a polarizing microscope, the birefringence of some of the spots actually excited by the laser beam were checked by placing a polarizer and phototube in the excitation beam after it passed through the sample and measuring the ratio of the transmitted light parallel and perpendicular to the incident polarization. This ratio was 150/1 or higher for all samples and is large enough to ensure that there was no distortion in the data due to birefringence in the samples. Fluorescence data were also collected on samples of pure PMMA and PVAc host materials. The fluorescence from these samples was negligible compared to the fluorescence from the naphthyl-containing samples.

D. Data Analysis. The experimental $r(t)$ and $G^s(t)$ were obtained from $I_{\parallel}(t)$ and $I_{\perp}(t)$ by the point-by-point calculations of eq 4 and 5. For an accurate comparison of the experimental curves with theoretical $G^s(t)$ curves calculated from eq 6–10, the experimental apparatus impulse response must be appropriately convolved with the theoretical $G^s(t)$. This was done by convolving theoretical expressions for $I_{\parallel}(t)$ and $I_{\perp}(t)$ (calculated from the theoretical $G^s(t)$ curves) with the instrument response function. For this system the response function was well approximated as a Gaussian with fwhm = 1.3 ns. The theoretical $G^s(t)$ with the convolution was then calculated from these new $I_{\parallel}(t)$ and $I_{\perp}(t)$ curves with eq 4 and 5.

E. R_0 and Lifetime Determinations. In order to unambiguously determine $\langle R_g^2\rangle^{1/2}$ by eq 8, it was necessary to independently determine R_0 and the fluorescence lifetime. R_0 can be affected by the host media. An unrealized difference in R_0 for the naphthalene chromophores in PMMA and PVAc would lead to an erroneous value for $\langle R_g^2\rangle^{1/2}$. A simple and accurate

way to determine R_0 is to measure $G^s(t)$ for excitation transport among chromophores randomly distributed in the desired media. R_0 is then determined by fitting the decay with an appropriate theory. The procedure has been discussed in detail previously.[6,33]

Samples containing various concentrations of 2-ethylnaphthalene in PMMA and PVAc were prepared as described above. The exact concentrations of 2-EN in the samples were determined by dissolving weighed pieces of the samples in THF and measuring the absorbance at 320 nm. Literature values for the densities of PMMA and PVAc[34] were used to calculate the volume. R_0 was determined to be 12.9 ± 0.4 Å in PMMA and in PVAc. This value compares favorably to that determined previously (13.0 ± 0.6 Å) for 2-EN in PMMA samples prepared by an entirely different method.[6] There is no difference in R_0 of 2-EN in the two host materials. Note that the value reported is R_0 and must be corrected as indicated in eq 10 when applied to static samples.

The fluorescence lifetime was determined to be 56 ± 4 ns by obtaining fluorescence decays of the various samples at magic-angle detection. The decays were well fit by a single exponential on the nanosecond time scale. No difference in lifetime was observed between PMMA and PVAc samples nor between those containing tagged polymer and 2-EN.

IV. Results and Discussion

Previous experiments have shown the utility of excitation transport experiments for the accurate determination of $\langle R_g^2 \rangle^{1/2}$ of polymer chains in amorphous solids.[7] The results presented here will further demonstrate the usefulness of these methods in the study of polymer blends. Time-resolved fluorescence depolarization spectroscopy is applied to monitor the rate of excitation transport among naphthyl chromophores attached to isolated guest chains (PMMA) in a host polymer (PVAc) with which they are immiscible. The immiscibility of the two polymers requires the tagged polymer to be present at an extremely low concentration. Monitoring the rate of excitation transport allows a quantitative determination of the $\langle R_g^2 \rangle^{1/2}$ for PMMA in PVAc and measurement of chain contraction. Concentration studies provide a simple and straightforward measure of the molecular miscibility of the two polymers.

A. Concentration Studies. Time-resolved fluorescence depolarization experiments were performed on samples made from copolymers 9-22 and 4-26 in both PMMA and PVAc hosts. (See Table I for copolymer characteristics.) In order to determine $\langle R_g^2 \rangle^{1/2}$ for the guest polymers, it is necessary not only that the chains are not in physical contact but also that they are separated to the extent that no interchain excitation transport can occur. For this purpose, studies of the extent of fluorescence depolarization as a function of tagged polymer concentration were performed. These studies show some interesting features.

It was determined previously[6,7] that the condition for no interchain transport is met for naphthyl-tagged PMMA of approximately 20 000 M_w at or below 0.38 wt % in PMMA. This was confirmed for the copolymers and host PMMA used in this study. To obtain physical separation of the tagged PMMA in PVAc, concentrations an order of magnitude lower than that required in PMMA host were necessary.

Figure 2 shows the change in $r(t)$ for the two tagged polymers in PVAc as a function of concentration. Interchain transport causes additional depolarization, resulting in a more rapidly decaying $r(t)$. As the concentration is lowered, $r(t)$ changes until a composition is reached where no interchain transport occurs. This happens between 0.092 and 0.055 wt % for copolymer 9-22 (Figure 2a) and between 0.034 and 0.019 wt % for copolymer 4-26 (Figure 2b). Measurements of mechanical and thermodynamic properties for blends of PVAc and PMMA containing 20% or more of the minor component show strong evidence of phase separation.[35-37] These data indicate that aggregation persists even at concentrations below 0.1 wt %. If there were no aggregation, interchain transport would stop at 0.38 wt % in PVAc as it did in PMMA.

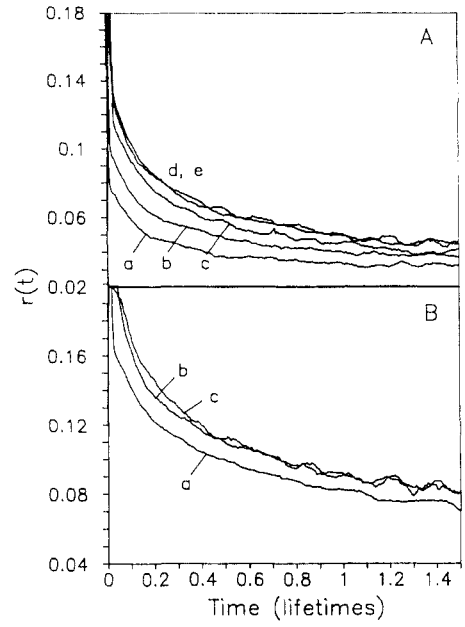

Figure 2. Effect of concentration on the excitation transport rate for tagged PMMA/PVAc blends. As the concentration of the 2-VN/MMA copolymer is decreased, the fluorescence anisotropy, $r(t)$, changes until a concentration is reached where no interchain excitation transport can occur. (A) Copolymer 9-22/PVAc at copolymer concentrations: (a) 0.55, (b) 0.18, (c) 0.092, (d) 0.055, and (e) 0.026 wt %. (B) Copolymer 4-26/PVAc at copolymer concentrations: (a) 0.034, (b) 0.019, and (c) 0.007 wt %. Note that for the higher molecular weight copolymer a lower concentration is required to ensure the chains are isolated.

As described in section III, the samples were prepared by molding blends at temperatures above the glass transition temperature of the host polymers. The amount of time the polymer blend was subjected to the high temperature and subsequent cooling to T_g and to room temperature were all rather short times compared to that of macromolecular diffusion. Thus, one might expect a competition between the equilibrium state of the mixture and kinetics to reaching this equilibrium in samples such as these. It is possible that the morphology of these blends is not necessarily that of a thermodynamic equilibrium mixture at room temperature. The degree of mixing may reflect that of the blend at the higher temperatures.

Fluorescence depolarization due to electronic excitation transport between chains can provide an extremely sensitive test of polymer miscibility at the molecular level. Aggregation, or perhaps more accurately, nonstatistical distributions of only two or three chains can be detected. Figure 3 demonstrates this using $G^s(t)$ calculations for excitation transport betwen chromophores randomly distributed in a sphere.[8] The upper curve is for 20 chromophores randomly distributed in a sphere of 40 Å (R_0' = 12.3 Å). The lower curve is for a sphere of twice this volume but the same chromophore density. Even though the chromophore density is unchanged, the energy transport is faster. For finite volume systems, increasing the volume and the number of chromophores proportionally results in a more rapid decay of $G^s(t)$ because there are more chromophores available to accept the excitation and

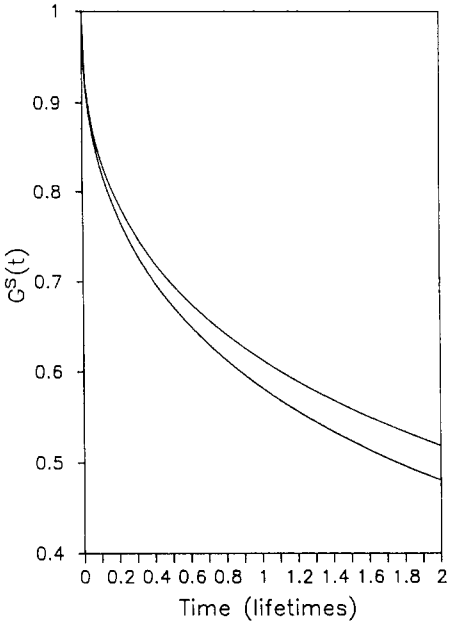

Figure 3. Model calculation demonstrating the effect aggregation can have on the excitation transport rate. Shown are calculated $G^s(t)$ curves for 20 chromophores (R_0' = 12.3 Å) randomly distributed in a sphere of 40 Å (upper) and 40 chromophores randomly distributed in a sphere of 50.4 Å (lower). In both cases, the chromophore density is the same, but the volumes differ by a factor of 2. The spheres are simple models for tagged polymer chains. Although the correct chromophore distribution function is not employed, the calculations show that aggregation of only two chains would cause an effect of the order observed in Figure 2.

also because edge effects, which decrease the transport rate, become less significant.

The shape of the decays in Figure 3 is not the same as those in the polymer data. This is because a random distribution function is not adequate to describe the spatial distribution of chromophores attached to a polymer chain. This simple model, although not containing the correct distribution for chromophores on polymer chains, shows that aggregation of two tagged chains, such as those used in these experiments, would cause an effect of the degree seen in Figure 2.

In fact, this model may even underestimate the effect of micro-phase separation on the excitation transport dynamics. If two tagged chains were closely aggregated, there would be some amount of chain entanglement. This would result in an increase in the chromophore density and an even faster decay of $r(t)$.

The presence or lack of micro-phase separation can also be seen in the shapes of the anisotropy decays in Figure 2. This can be understood by considering the chromophore distributions. The chromophore pair-correlation function associated with a phase-separated domain of tagged chains is not the same as that for an isolated chain. The spatial distribution of chromophores attached to the same chain would be described by a Gaussian pair-correlation function (eq 6). However, chromophores on different chains would be spatially uncorrelated. Excitation transport dynamics are highly dependent on the spatial distribution of the chromophores. The difference in the distribution of chromophores in a phase-separated domain relative to that on isolated chains would lead to a difference in the rate of excitation transport. This would be reflected in the shape of the anisotropy curves.

Indeed, the anisotropy decays for the higher concentrations of tagged chains do have a different general shape than those for the lowest concentrations. This can be seen most clearly in Figure 2a. Furthermore, as is shown in the next section, the experimental $G^s(t)$ curves derived from the lowest concentration $r(t)$ data are very well fit by using the Gaussian pair-correlation function appropriate for isolated chains. This would not be true when phase separation is present, due to the change in the shape of the decays.

Another interesting effect is seen in the concentration dependence. A lower concentration was necessary to achieve isolated chains in PVAc for the 26 000 M_w chains (copolymer 4-26) as compared to the 22 700 M_w chains (copolymer 9-22). It is well-known that the molecular weights of blend components can have a significant effect on miscibility, especially when the two components have a large difference in molecular weight. The observation of this effect for two guest copolymers that differ in average length by only 33 monomer units is remarkable. It is possible that the difference in naphthyl content between the two copolymers could contribute to this effect. However, on the basis of $\langle R_g^2 \rangle^{1/2}$ data discussed below, this does not seem likely. Further experiments that make use of different molecular weight chains with equivalent chromophore densities could help quantify molecular weight effects on microphase separation.

B. $\langle R_g^2 \rangle^{1/2}$ Determination. As discussed in section II, to determine $\langle R_g^2 \rangle^{1/2}$ it is necessary to assess the amount of depolarization due to molecular motions and the polarization properties of the electronic transition excited. This was done by measuring the time-dependent fluorescence anisotropies for copolymer I in PMMA and PVAc. In these samples there was neither inter- or intrachain excitation transport. Since it was necessary to go to extremely low concentration to ensure that the copolymer I chains were in a pure PVAc environment, the signal-to-noise for this measurement was adequate but not good. It was clear that there was no significant difference in the anisotropies in the two hosts. Therefore, the anisotropy measured for copolymer I in PMMA was used in constructing all the $G^s(t)$ curves.

Figure 4 shows polarized fluorescence decays ($I_\parallel(t)$ and $I_\perp(t)$) for a 0.026 wt % copolymer 9-22/PVAc blend. The effect of excitation transport is seen in the convergence of the two decays with time. Figure 5 (lower curve) shows the time-dependent fluorescence anisotropy, $r(t)$, calculated from the data in Figure 4 by eq 5. (Note that lifetime effects are also removed by this procedure.) The upper curve is $r(t)$ obtained in the same manner for copolymer I and exhibits depolarization due only to molecular motion and time-independent sources. As discussed in section II, to observe the effects due solely to excitation transport, it is necessary to take the ratio of the two anisotropies. Experimental $G^s(t)$ curves, which give the probability that initially excited chromophores are excited at time t, were constructed in this manner from the $r(t)$ data.

Figure 6 shows experimental $G^s(t)$ curves for blends of copolymer 9-22 in PMMA and PVAc. Figure 7 illustrates the results for copolymer 4-26 in the two hosts. In both cases, there is a marked increase in the rate of excitation transport when the tagged polymers are placed in PVAc instead of PMMA. As discussed in the Introduction, this indicates an increase in the local concentration of the naphthyl chromophores that would occur as the result of chain contraction.

Also shown in Figures 6 and 7 are the best fit $G^s(t)$ curves calculated according to the theory in section II. Variation of the single adjustable parameter, the statis-

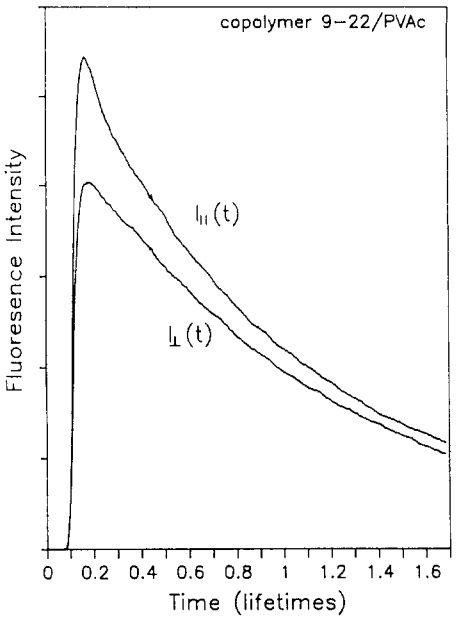

Figure 4. Polarized fluorescence decays for a copolymer 9-22/PVAc blend for detection parallel ($I_{\parallel}(t)$) and perpendicular ($I_{\perp}(t)$) to the polarization of the excitation beam. The sample is copolymer 9-22 (0.087 mole fraction 2-VN, 22 700 M_w) in an ~167 000 molecular weight PVAc host. The copolymer concentration is 0.026 wt %.

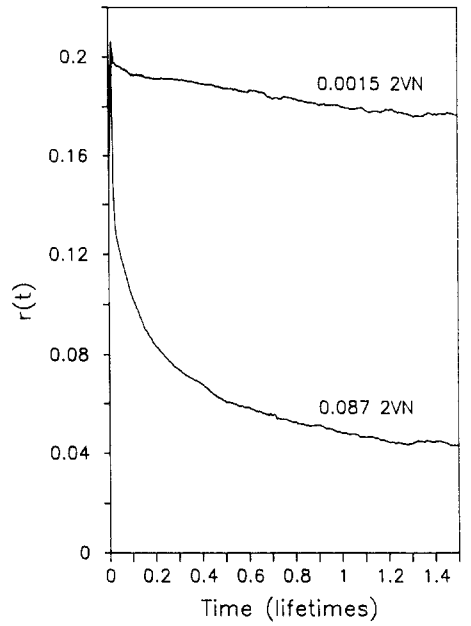

Figure 5. Time-dependent fluorescence anisotropies for 2-VN/MMA copolymers in PVAc. The upper curve is for a copolymer with a very small mole fraction (0.0015) of 2-VN (copolymer I). Excitation transport does not occur, and the time dependence is due to rotational depolarization. The lower curve is a copolymer 9-22/PVAc blend. Here, the time-dependent depolarization is due to both excitation transport and rotational motion.

tical segment length (a), results in $\langle R_g^2\rangle^{1/2}$ of 40 and 34 Å for copolymer 4-26 in PMMA and PVAc, respectively, and of 39 and 34 Å for copolymer 9-22 in PMMA and PVAc. These results are summarized in Table II.

Also given in Table II are values of $\langle R_g^2\rangle^{1/2}$ for PMMA under Θ conditions. These were calculated from reported literature values of unperturbed chain dimensions from light scattering measurements on PMMA in various solvents at the Θ point.[38] As initially proposed by Flory[39] and confirmed by neutron scattering[13] and excitation transport experiments,[7] the ensemble averaged conformation of a polymer chain is the same in the bulk solid and in Θ solution. As seen before,[7] the values obtained by these excitation transport experiments for bulk PMMA are in quantitative agreement with the Θ condition values.

The decrease in $\langle R_g^2\rangle^{1/2}$ observed in changing from the PMMA host to PVAc is significant; 15% for copoly-

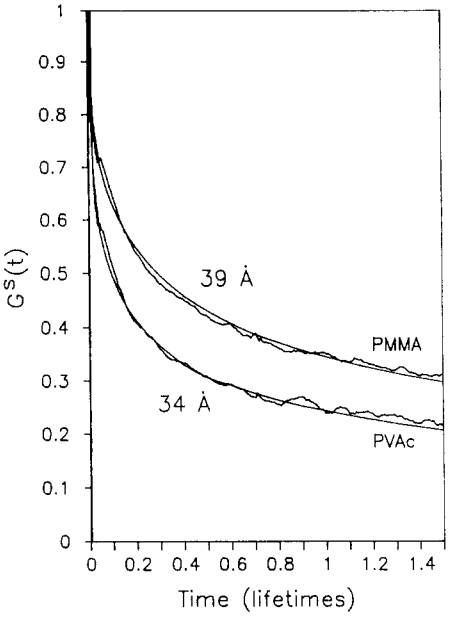

Figure 6. Experimental $G^s(t)$ and theoretical fits for copolymer 9-22 in PVAc and in PMMA. The upper data curve is for the PMMA blend, and the lower is for the PVAc blend. $G^s(t)$ decays faster in PVAc due to contraction of the copolymer chains. Also shown are theoretical $G^s(t)$ curves calculated by using the theory of section II for a 22 700 M_w PMMA chain with 20 naphthyl groups. The best fits result in $\langle R_g^2\rangle^{1/2}$ of 39 Å in PMMA and 34 Å in PVAc. The result for the copolymer 9-22/PMMA blend is in excellent agreement with light scattering measurements of $\langle R_g^2\rangle^{1/2}$ for PMMA in Θ solvents.

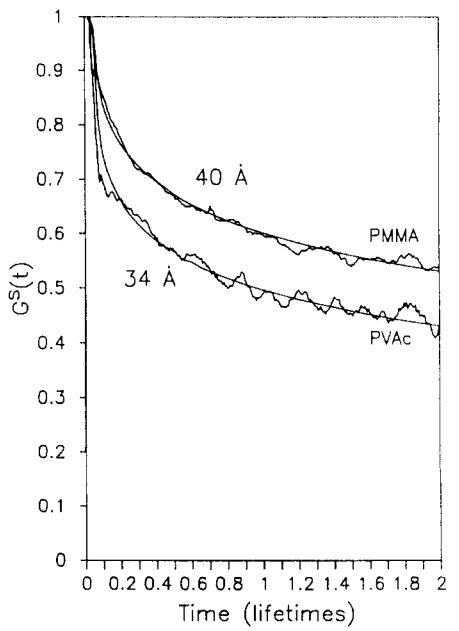

Figure 7. Experimental $G^s(t)$ and theoretical fits for copolymer 4-26 in PVAc and PMMA. Chain contraction in PVAc leads to an increased rate of excitation transport. The theoretically calculated $G^s(t)$ curves yield $\langle R_g^2\rangle^{1/2}$ of 40 Å in PMMA and 34 Å in PVAc. The result in PMMA is in close agreement with light scattering measurements of $\langle R_g^2\rangle^{1/2}$ for PMMA in Θ solvents.

Table II
Summary of Results

copolymer	$\langle R_g^2\rangle^{1/2}$, Å: PVAc[a]	PMMA[a]	θ solv[b]	α: R_g(PVAc)/R_g(PMMA)
4-26	34 ± 3	40 ± 3	41 ± 4	0.85 ± 0.03
9-22	34 ± 3	39 ± 3	38 ± 4	0.87 ± 0.03

[a] Measured by excitation transport. [b] From tabulated results of light scattering measurements.[36]

mer 4-26 and 13% for copolymer 9-22. The chain contraction can be expressed in terms of the expansion coefficient α, which is defined as the as the ratio of the measured radius of gyration and its value near θ conditions. The values of α for copolymers 4-26 and 9-22 in PVAc are 0.85 and 0.87, respectively. These values are also listed in Table II. The equivalence of the percent change for two copolymers of essentially the same molecular weight, but over a factor of 2 difference in naphthyl content indicates there is no significant effect due to the presence of the chromophores.

A note is necessary on the error associated with these measurements. As previously, we have assigned an absolute error of ±3 Å to the $\langle R_g^2\rangle^{1/2}$ values.[7] As discussed in the previous paper, this error estimate is almost entirely due to possible errors in the determination of the tagging fraction and the molecular weight. Considering the concurrence of the measurements with the θ condition values, this estimate is probably generous.

Any systematic errors in characterizing a copolymer is the same regardless of which host it is placed in. Comparisons between the same copolymer in different host materials can provide a very accurate determination of chain contraction or expansion. The magnitude of the change observed has a much smaller relative error associated with it which is only determined by random errors in data acquisition. The fluorescence depolarization data are extremely reproducible within each sample and between samples of the same type, the signal-to-noise being limited only by the number of laser shots accumulated. Thus, the relative error in α is quite low.

The accuracy of these radius of gyration measurements rests on the validity of using Gaussian chain statistics to describe flexible polymers in a collapsed state. Strictly speaking, a perturbed chain is not exactly modeled by a random walk. However, just as θ condition polymers of different stiffness can be described by the random walk model using different statistical segment lengths, an expanded or contracted chain may be reasonably modeled by a random walk with a modified segment (step) length.

Consider an ensemble of chains in a medium having less favorable polymer–medium interactions than in a θ condition solvent. The chains, on average, will contract. A chain can still be considered to be freely jointed, but it is now executing a biased walk rather than a random walk. There will be a tendency for the segments of the chain to avoid the medium. The bias will cause a more rapid turn toward the coil center than in a random walk.

If we imagine a segment being constructed by connecting monomers one after another, a segment that starts to "head" into the unfavorable medium will have its distribution of monomer units skewed in a manner that will turn it around more rapidly than in a θ condition medium. The effect is that segments that head into the unfavorable medium have a segment length that is shorter than the average length in a θ condition medium. In a medium that has more favorable interactions with the polymers than a θ condition medium, segments that head into the favorable medium will have a length that is longer than the average length in a θ condition medium.

We can replace a detailed description of such a biased walk by a random walk with a modified step length. The statistical segment length in a θ condition medium a becomes an effective segment length a_{eff}. In an unfavorable medium, a_{eff} is shorter than a. In analyzing excitation transport data, the equations given in section II are used, with a single adjustable parameter, a_{eff}.

While a biased walk spatial distribution function is different from a random walk distribution function, the second moment ($\langle R_g^2\rangle^{1/2}$ is not particularly sensitive to the details of the distribution function if the bias is not too great. For very collapsed chains, it may be desirable to replace eq 6 with a distribution function that describes the collapsed state more accurately. However, due to the sensitivity of excitation transport to the spatial distribution of the chromophores, if a Gaussian distribution function is no longer applicable, it should become apparent in the shapes of the $G^s(t)$ decays. For the data presented here, the theoretical $G^s(t)$ curves calculated by using the Gaussian segment distribution function match the shape of the experimental decays extremely well, indicating that the random walk model with a modified step length provides a valid description of the spatial distribution.

It is interesting to compare the results obtained here for PMMA/PVAc to those obtained for other systems by other methods. As mentioned in the Introduction, there has been considerable interest in experimentally observing changes in average chain conformation with environment in both polymer solutions and solids. Light scattering has been used extensively to measure $\langle R_g^2\rangle^{1/2}$ and hydrodynamic radii for macromolecules in dilute solution.[9] Chain expansions of over 50% have been observed for many polymers in good solvents. Chain collapse of very large molecular weight polymers has been measured in solutions where the temperature is lowered below the θ point.[10,11] For example, polystyrene in methyl acetate shows a 10–15% decrease in $\langle R_g^2\rangle^{1/2}$ at 9 °C below the θ temperature.[11b]

Several researchers have used small-angle neutron scattering to measure polymer interaction parameters and chain expansion in a number of miscible polymer blends.[14-16] Chain expansion ranging from a few to 50% relative to θ condition has been observed. SANS has also been used to investigate miscible blends that exhibit an upper miscibility gap. As the temperature is raised, a decrease in the radius of gyration of the minor component is observed.[14c] The results presented above for PMMA/PVAc are the first measurements of $\langle R_g^2\rangle^{1/2}$ and chain collapse in a mixture of two incompatible polymers.

The change in $\langle R_g^2\rangle^{1/2}$ we have observed for PMMA in PVAc is consistent in magnitude with the changes observed for other polymers under non-θ conditions. The direction of the change is also appropriate; chain collapse is expected for an environment with which the guest polymer is incompatible. To put these measurements in perspective, it is informative to calculate α expected for fully collapsed PMMA chains of the appropriate molecular weights.

This can be done by using the theory for chain collapse in solvents commonly known as the "blob theory".[10,11] This theory models a polymer chain of N monomers as a succession of blobs, each containing N_c monomers. The chain obeys Gaussian statistics within each blob. However, the necklace of N/N_c blobs has an

expanded structure above or a collapsed structure below the Θ point.

In the poor solvent limit (significant chain contraction), the expansion factor for the radius of gyration is expressed as

$$\alpha = 1.161(N/N_c)^{-1/6} \quad (12)$$

For a fully collapsed chain, $N_c = 1$.

The values of α for fully collapsed chains of 22 700 and 26 000 molecular weight are then 0.47 and 0.46, respectively. Given this limit and that of $\alpha = 1$ for unperturbed chains, one can say that the PMMA chains are 25–28% collapsed when dispersed in PVAc. The degree of chain collapse relative to the fully collapsed state should be a useful way of characterizing the changes in thermodynamic interactions in solid blends as the guest polymer is dispersed in various host polymers.

V. Concluding Remarks

The experiments and results presented in this paper represent a distinct contribution to the study of polymeric materials. These are the first measurements of average chain conformation in a solid polymer blend where the components are strongly immiscible. In addition, the sensitivity to aggregation of a small number of polymer chains allows the study of such properties as critical concentrations and the size of micro-phase-separated domains. Since very few polymers are miscible, techniques utilizing electronic excitation transport phenomena open the door to quantitative study of microscopic structure and interactions in a wider class of macromolecular materials.

Acknowledgment. This work was supported by the Department of Energy, Office of Basic Energy Sciences (DE-FG03-84ER13251). Additional equipment support was provided by the National Science Foundation, Division of Materials Research (DMR 87-18959). We also thank the members of the Stanford Center for Materials Research Polymers Thrust Program, especially Professor C. W. Frank, for helpful discussions.

Registry No. (MMA)(2-VN) (copolymer), 53640-71-4; PMMA, 9011-14-7; PVAc, 9003-20-7.

References and Notes

(1) (a) Fitzgibbon, P. D.; Frank, C. W. *Macromolecules* **1982**, *15*, 733. (b) Gelles, R.; Frank, C. W. *Macromolecules* **1983**, *16*, 1448. (c) Semerak, S. N.; Frank, C. W. *Can. J. Chem.* **1983**, *63*, 1328.
(2) (a) Morawetz, H.; Amrani, F. *Macromolecules* **1978**, *11*, 281. (b) Morawetz, H. *Pure Appl. Chem.* **1980**, *52*, 277.
(3) Wang, F. W.; Lowry, R. F. *Polymer Prepr. (Am. Chem. Soc., Div. Polym. Chem.)* **1982**, *23*, 205.
(4) Ediger, M. D.; Fayer, M. D. *J. Phys. Chem.* **1984**, *88*, 6109.
(5) Peterson, K. A.; Stein, A. D.; Fayer, M. D. In *Molecular Dynamics in Restricted Geometries*; Klafter, J., Drake, J. M., Eds.; Wiley: New York, 1989.
(6) Ediger, M. D.; Domingue, R. P.; Peterson, K. A.; Fayer, M. D. *Macromolecules* **1985**, *18*, 1182.
(7) Peterson, K. A.; Zimmt, M. B.; Linse, S.; Domingue, R. P.; Fayer, M. D. *Macromolecules* **1987**, *20*, 168.
(8) Peterson, K. A.; Fayer, M. D. *J. Chem. Phys.* **1986**, *85*, 4702.
(9) *Light Scattering from Polymer Solutions*; Huglin, M. B. Ed.; Academic Press: New York, 1972.
(10) Vidakovic, P.; Rondelez, F. *Macromolecules* **1984**, *17*, 418.
(11) (a) Park, I. H.; Wang, Q.-W.; Chu, B. *Macromolecules* **1987**, *20*, 1965. (b) Chu, B.; Park, I. H.; Wang, Q.-W.; Wu, C. *Macromolecules* **1987**, *20*, 2833. (c) Park, I. H.; Fetters, L.; Chu, B. *Macromolecules* **1988**, *21*, 1178.
(12) Cotton, J. P.; Decker, D.; Benoit, H.; Farnoux, B.; Higgins, J.; Jannik, G.; Ober, R.; Picot, C.; des Cloizeaux, J. *Macromolecules* **1974**, *7*, 863.
(13) Kirste, R. G.; Kruse, W. A.; Ibel, K. *Polymer* **1975**, *16*, 120.
(14) (a) Kruse, W. A.; Kirste, R. G.; Haas, J.; Schmitt, B. J.; Stein, D. J. *Makromol. Chem.* **1976**, *177*, 1145. (b) Schmitt, B. J.; Kirste, R. G.; Jelenic, J. *Makromol. Chem.* **1980**, *181*, 1655. (c) Jelenic, J.; Kirste, R. G.; Oberthür, R. C.; Schmitt-Strecker, S.; Schmitt, B. J. *Makromol. Chem.* **1984**, *185*, 129.
(15) Wignall, G. D.; Child, H. R.; Li-Aravena, F. *Polymer* **1980**, *21*, 131.
(16) Ito, H.; Russell, T. P.; Wignall, G. D. *Macromolecules* **1987**, *20*, 2213.
(17) Strazielle, C.; Benoit, H. *Macromolecules* **1975**, *8*, 203.
(18) Schelten, J.; Wignall, G. D.; Ballard, D. G. H.; Longman, G. W. *Polymer* **1977**, *18*, 1111.
(19) (a) Bates, F. S.; Wignall, G. D.; Koehler, W. C. *Phys. Rev. Lett.* **1985**, *55*, 2425. (b) Wignall, G. D.; Bates, F. S. *Makromol. Chem., Makromol. Symp.* **1988**, *15*, 105.
(20) Yang, H.; Hadziioannou, G.; Stein, R. S. *J. Polym. Sci., Polym. Phys. Ed.* **1983**, *21*, 159.
(21) Russel, T. P.; Stein, R. S. *J. Polym. Sci., Polym. Phys. Ed.* **1982**, *20*, 1593.
(22) Gochanour, C. R.; Andersen, H. C.; Fayer, M. D. *J. Chem. Phys.* **1979**, *70*, 4254.
(23) Fredrickson, G. H. *J. Chem. Phys.* **1989**, in press.
(24) Galinin, M. D. *Tr. Fiz. Inst. I. P. Pavlova* **1950**, *5*, 341.
(25) Yamakawa, M. *Modern Theory of Polymer Solutions*; Harper and Row: New York, 1971; Chapter 2.
(26) In previous discussions of this theory (ref 5, 7, and 8), A, the volume of a sphere of radius $a/2$, was inadvertently neglected in the text in the denominator of the expression for the probability of finding a chromophore on the same segment as the initially excited chromophore (eq 7). However, this normalization was properly used in the calculations that were presented.
(27) (a) Förster, Th. *Ann. Phys. (Leipzig)* **1948**, *2*, 55. (b) Förster, Th. *Z. Naturforsch., A: Astrophys. Phys. Phys. Chem.* **1949**, *4*, 321.
(28) Haan, S. W.; Zwanzig, R. *J. Chem. Phys.* **1978**, *68*, 1879.
(29) (a) Huber, D. L. *Phys. Rev. B* **1979**, *20*, 2307. (b) Huber, D. L. *Phys. Rev. B* **1979**, *20*, 5333.
(30) Baumann, J.; Fayer, M. D. *J. Chem. Phys.* **1986**, *85*, 4087.
(31) (a) Gochanour, C. R.; Fayer, M. D. *J. Phys. Chem.* **1981**, *85*, 1989. (b) Fredrickson, G. H.; Andersen, H. C.; Frank, C. W. *Macromolecules* **1983**, *16*, 1456.
(32) Fox, T. G.; Kinsinger, J. B.; Mason, H. F.; Schuele, E. M. *Polymer* **1962**, *3*, 71.
(33) Peterson, K. A.; Zimmt, M. B.; Fayer, M. D.; Jeng, Y. H.; Frank, C. W. *Macromolecules* **1989**, *22*, 874.
(34) Lindemann, M. K.; Wunderlich, W. In *Polymer Handbook*; Brandrup, J., Immergut, E. H., Eds.; Wiley-Interscience: New York, 1975; Sections V-8 and V-9.
(35) Slonimskii, G. L. *J. Polym. Sci. (Prague Symp.)* **1958**, *30*, 625.
(36) Ichihara, S.; Komatsu, A.; Hata, T. *Polym. J.* **1971**, *2*, 640.
(37) von Jenckel, E.; Herwig, H. U. *Kolloid-Z.* **1956**, *148*, 57.
(38) Jurata, M.; Tsunashima, Y.; Iuama, M.; Kamada, K. In *Polymer Handbook*; Brandrup, J., Immergut, I. H., Eds.; Wiley-Interscience: New York, 1975; p IV-38.
(39) (a) Flory, P. J. *Principles of Polymer Chemistry*; Cornell University Press: Ithaca NY, 1953; p 602. (b) Hayashi, H.; Flory, P. J.; Wignal, G. D. *Macromolecules* **1983**, *16*, 1328.